Biochimica et Biophysica Acta 1838 (2014) 2099–2104

Contents lists available at ScienceDirect

Biochimica et Biophysica Acta

journal homepage: www.elsevier.com/locate/bbamem

The structure of *Lactobacillus brevis* surface layer reassembled on liposomes differs from native structure as revealed by SAXS

Inkeri Kontro [a,*], Susanne K. Wiedmer [b], Ulla Hynönen [c], Paavo A. Penttilä [a], Airi Palva [c], Ritva Serimaa [a]

[a] Department of Physics, P.O.B. 64, 00014 University of Helsinki, Finland
[b] Department of Chemistry, P.O.B. 55, 00014 University of Helsinki, Finland
[c] Department of Veterinary Biosciences, P.O.B. 66, 00014 University of Helsinki, Finland

ARTICLE INFO

Article history:
Received 24 January 2014
Received in revised form 3 April 2014
Accepted 23 April 2014
Available online 4 May 2014

Keywords:
SAXS
Liposomes
S-layer
Lactobacillus brevis

ABSTRACT

The reassembly of the S-layer protein SlpA of *Lactobacillus brevis* ATCC 8287 on positively charged liposomes was studied by small angle X-ray scattering (SAXS) and zeta potential measurements. SlpA was reassembled on unilamellar liposomes consisting of 1-palmitoyl-2-oleyl-sn-glycero-3-phosphocholine and 1,2-dioleoyl-3-trimethylammonium-propane, prepared by extrusion through membranes with pore sizes of 50 nm and 100 nm. Similarly extruded samples without SlpA were used as a reference. The SlpA-containing samples showed clear diffraction peaks in their SAXS intensities. The lattice constants were calculated from the diffraction pattern and compared to those determined for SlpA on native cell wall fragments. Lattice constants for SlpA reassembled on liposomes ($a = 9.29$ nm, $b = 8.03$ nm, and $\gamma = 84.9°$) showed a marked change in the lattice constants b and γ when compared to those determined for SlpA on native cell wall fragments ($a = 9.41$ nm, $b = 6.48$ nm, and $\gamma = 77.0°$). The latter are in good agreement with values previously determined by electron microscopy. This indicates that the structure formed by SlpA is stable on the bacterial cell wall, but SlpA reassembles into a different structure on cationic liposomes. From the (10) reflection, the lower limit of crystallite size of SlpA on liposomes was determined to be 92 nm, corresponding to approximately ten aligned lattice planes.

1. Introduction

The outmost layer of the cell envelope of many bacteria and archaea is a crystalline surface protein (S) layer. S-layers are composed of identical protein or glycoprotein subunits with molecular weights of 40–200 kDa, which form a regular, porous lattice with oblique (p1, p2), square (p4) or hexagonal (p3, p6) symmetry. S-layer proteins attach to the cell surface by non-covalent interactions. They reassemble spontaneously in solution and on solid supports by an entropy-driven process [1]. S-layers have varying functions in vivo, ranging from structural support of the cell shape to functions as molecular sieves, as binding sites for large molecules or as mediators of bacterial adhesion [2].

The detection and characterization of the S-layer lattice relies still largely on electron microscopy [1,3]. S-layers have also been studied by atomic force microscopy [4–6] and recently by small-angle X-ray scattering [7–9]. SAXS provides information on the lattice constants and crystallite size averaged over the whole volume of the sample, whereas microscopic methods provide information only about local details. SAXS can be used to study biological samples suspended in buffer solution, and temperature control of samples is possible. Unlike electron microscopy, sample preparation for SAXS experiments does not require chemical fixation, staining, freezing or dehydration of the sample, and with synchrotron sources, measurement times are reduced to minutes.

Liposomes are hollow aggregate structures that phospholipids form when dispersed in aqueous solutions. The use of liposomes in biomedical and medical applications is highly diverse. They can be used, for instance, to enhance drug delivery by encapsulating biologically active molecules in the internal aqueous lumen or in the lipid bilayer [10,11]. S-layer proteins have successfully been reassembled on lipid surfaces, both on planar films and on liposomes [12]. S-layer coatings reduce the leakage of the active molecules from liposomes, and have been shown to stabilize liposomes against e.g. mechanical and thermal stress [13], treatments with pancreatic extract and bile salts, and changes in the environmental pH [14]. Further, S-layers reassembled on liposomes have been suggested to function as immobilization matrices for functional molecules [15] or as templates for constructing silica-enhanced cages [16]. The S-layer protein of *Lactobacillus acidophilus* ATCC 4356 crystallizes readily on negatively charged phospholipid monolayers, but forms only small patches on phosphocholine monolayers [17]. On the other hand, Hollmann et al. showed that the S-layer proteins of *Lactobacillus kefir* JCM 5818 and *Lactobacillus brevis* ATCC 14869 reassemble on positively charged liposomes [14].

L. brevis ATCC 8287 is a putatively probiotic organism that has been suggested as a possible platform to present vaccine antigens [7,18,19]. Its S-layer protein SlpA, a 46 kDa protein, facilitates the bacterium's

* Corresponding author. Tel.: +358 92941 50627.
E-mail address: inkeri.kontro@helsinki.fi (I. Kontro).

http://dx.doi.org/10.1016/j.bbamem.2014.04.022
0005-2736/

adhesion to human intestinal epithelia [20]. SlpA is a thermally highly stable protein [21] which forms a crystalline layer with oblique symmetry. Lattice constants for the native S-layer were $a = 9.39$ nm, $b = 6.10$ nm and $\gamma = 79.8°$, as determined by electron microscopy [22].

In this study, we reassembled SlpA on the surface of positively charged liposomes composed of 1-palmitoyl-2-oleyl-*sn*-glycero-3-phosphocholine (POPC) and 1,2-dioleoyl-3-trimethylammonium-propane (chloride salt) (DOTAP). Phosphocholines are zwitterionic phospholipids which are the major constituent of biological membranes, and DOTAP was chosen in order to have model vesicles with a net positive charge. Cationic DOTAP liposomes are much used as transfection agents for gene delivery, due to the spontaneously formed stable complexes when mixed together with DNA [23].

The reassembly was studied by SAXS and the observed data were complemented with size and surface charge measurements by dynamic light scattering (DLS) and zeta potential measurements, respectively. The lattice constants for the S-layer reassembled on liposomes were compared to those of the native S-layer on *L. brevis* ATCC 8287 cell wall fragments. To our knowledge, SAXS has not previously been used to characterize S-layer reassemblies on liposomes.

2. Materials and methods

2.1. Purification of the S-layer protein and preparation of native cell wall fragments

The gene encoding the S-layer protein SlpA of *L. brevis* ATCC 8287 was expressed in *Escherichia coli* BL21 (DE3), and recombinant SlpA (rSlpA) with an N-terminal hexahistidine tag was purified under denaturing conditions as previously described [22]. After the affinity purification, dialyzed rSlpA was centrifuged for 20 min (15,000 *g*) at +4 °C and the supernatant was stored at −86 °C. Before liposome preparation, the protein in 4.24 mM sodium phosphate buffer at pH 7.4 (ionic strength of 10 mM) was centrifuged for 30 min (27,000 *g*), and the supernatant (190 μg/ml) was used for the preparation of liposomes.

For the preparation of crude cell wall fragments, *L. brevis* ATCC 8287 cells were grown in 1 L of MRS medium (Difco, Detroit, MI, USA) at 37 °C overnight. The cells were collected by centrifugation, washed once with 50 mM Tris-HCl (pH 7.5), resuspended and disrupted by French Pressure Cell Press (SLM Instruments Inc., IL, USA). The lysate was centrifuged at 3000 *g* for 5 min at +4 °C, washed five times with 50 mM Tris-HCl (pH 7.5) and resuspended in 50 mM Tris-HCl at pH 7.5.

2.2. Liposome preparation

Lipids used for liposome preparation were 1-palmitoyl-2-oleyl-*sn*-glycero-3-phosphocholine (POPC) and 1,2-dioleoyl-3-trimethylammonium-propane (chloride salt) (DOTAP) purchased from Avanti Polar Lipids (Alabaster, Alabama, US).

The lipids were dissolved in chloroform prior to liposome preparation. POPC was mixed with DOTAP at a ratio of 70:30 mol%. Chloroform was evaporated under nitrogen flow and further under vacuum for 1 h. The dry lipid film was rehydrated in 1.2 ml of 4.24 mM sodium phosphate buffer at pH = 7.5 (ionic strength of 10 mM) or in 1.2 mL of sodium phosphate buffer containing 190 μg/mL of SlpA. The total liposome concentration was 2 mM in both cases. Control liposomes (i.e. those lacking SlpA) were kept at 60 °C for an hour, with occasional mixing. SlpA-containing samples were kept under agitation for 180 min at room temperature.

Unilamellar vesicles were prepared by extrusion of multilamellar vesicles. The extrusion was done after the addition of SlpA to avoid the dilution of the protein sample. Due to the low transition temperature of the lipids (−2 °C for POPC [23] and 0 °C for DOTAP [24]), the extrusion could be performed at room temperature with an Avanti Mini Extruder using membranes with 50 nm and 100 nm pore sizes and repeated 19 or 21 times. The extruded samples were stored at +4 °C.

2.3. Zeta potential and size measurements

The size distribution and zeta potential of the liposomes were examined by Zetasizer Nano-ZS (Malvern Instruments Ltd, Worcestershire, UK). The samples lacking SlpA were diluted 20-fold and the samples containing SlpA 30-fold. DLS was measured at 20 °C using a helium–neon laser at the wavelength of 633 nm, detection angle of 173°, and the viscosity value was set at 1.0031 cP (for water). Measurements were repeated three times and an average intensity was calculated. Zeta potential measurements were done at 20 °C, and a dielectric constant of 80.4 (for water) and a viscosity value of 1.0031 cP (for water) were used in the calculations. The applied electric field strength was 150 V/cm. One run consisted of ten individual measurements and the results were expressed as the mean values of three runs.

2.4. SAXS measurements

SAXS measurements of the liposome samples were conducted on beamline I911-SAXS at MAX-lab, Lund, Sweden [25]. The sample-to-detector distance was 1.9 m and the wavelength $\lambda = 0.091$ nm. The flow-through cell set-up was used, with sample volumes of 30 μL. The measurement times were 10 x 1 min. The sample was oscillated slowly during the measurement to subject a larger sample volume to the beam, minimizing radiation damage. The damage was monitored by comparing the first measurement with the later ones (see supporting information).

The angular calibration was done with a silver behenate standard sample, yielding a q-range of $0.085\ \text{nm}^{-1} < q < 4.9\ \text{nm}^{-1}$, where q is the length of the scattering vector described as $q = (4\pi\sin\theta) / \lambda$, with θ being half of the scattering angle. The calibration and data reduction were done by the software Bli911-4 available at the beamline. The integrated intensity was normalized by transmission and the background scattering was subtracted.

SAXS measurements of native bacterial cell wall fragments were performed using a rotating anode X-ray tube (UltraX18S, Rigaku) with 1.6 m sample to detector distance and a Pilatus 1 M detector. The radiation ($CuK_{\alpha 1}$, $\lambda = 0.154$ nm) was focused in the vertical direction by an elliptical mirror and monochromatized and focused in the horizontal direction using an asymmetrically cut, bent Si-111 crystal. The sample was pelleted by centrifugation and measured in a metal ring (thickness of 1 mm) sealed on both sides with Mylar foil. The measurement time was 10 h. The angular calibration was done with a silver behenate sample, and the q-range was found to be 0.20–4.2 nm^{-1}. No normalization by transmission was done for these data.

3. Results and discussion

3.1. Diameter and zeta potential

The adsorption of SlpA on model liposomes was studied using cationic liposomes composed of 70/30 mol% POPC/DOTAP. The liposomes were prepared by extrusion and membranes with two different pore sizes, 50 and 100 nm. The purpose was to investigate whether the curvature of the liposome would affect the adsorption of the protein onto the membrane surface.

The diameter distribution of both SlpA-containing and reference liposome samples was measured by DLS (Fig. 1). The reference liposome sample extruded through the 100 nm membrane had a maximum in volume probability at 128 nm, while the corresponding SlpA-containing liposome sample had a maximum in volume probability at 148 nm. The reference liposome sample extruded through the 50 nm membrane gave a slightly smaller diameter with a maximum in volume probability at 98 nm. The corresponding SlpA-containing liposome sample had also in this case a larger diameter than the crude liposome; however, the volume probability distribution of the sample showed two distinct peaks with maximums at diameters 27 nm and 113 nm,

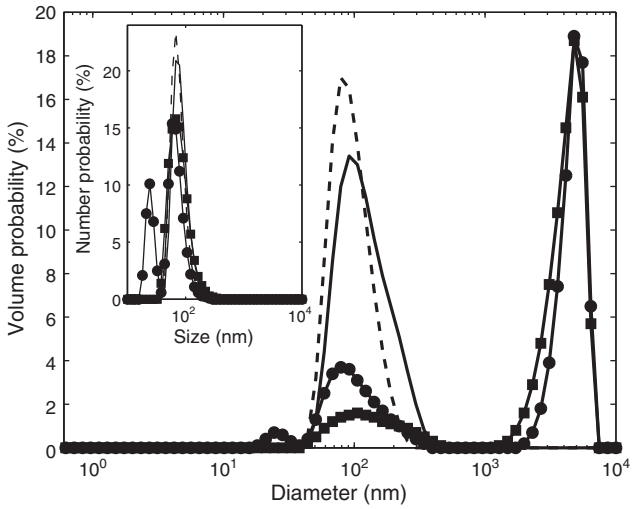

Fig. 1. Diameter distribution of SlpA-containing and reference liposomes determined by DLS. Reference liposomes extruded through 100 nm membranes (solid line), reference liposomes extruded through 50 nm membranes (dashed line), SlpA-containing liposomes extruded through 100 nm membranes (■) and SlpA-containing liposomes extruded through 50 nm membranes (●) were analyzed by DLS. Shown are volume probability (main image) and number probability (inset).

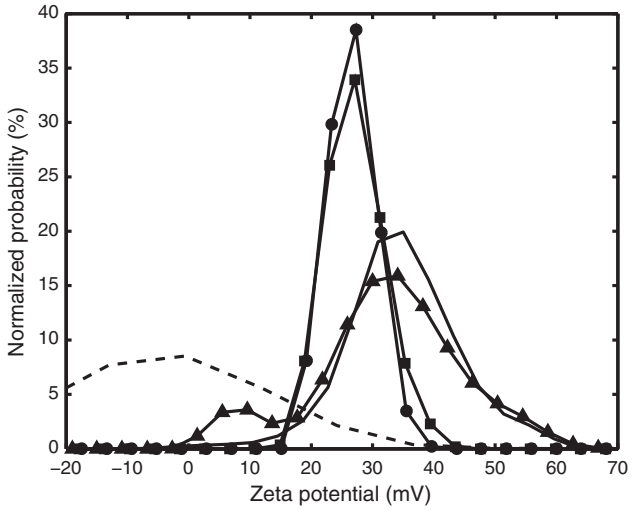

Fig. 2. Zeta potentials of liposome samples. Shown are the zeta potentials of reference liposomes extruded through 100 nm membranes (solid line) or 50 nm membranes (▲), of SlpA-containing liposomes extruded through 100 nm membranes (■) or 50 nm membranes (●) and the zeta potential of SlpA (dashed line).

with the latter species being more prominent. The peak at smaller values is likely due to small protein aggregates.

Both SlpA-containing samples showed, in addition to the intensity maximum corresponding to the extruded liposomes, also a broad and ill-defined peak at higher values. This was most probably due to the presence of a small amount of contamination of the sample. One possible explanation is that if protein was dislodged in the extrusion process, few but large protein aggregates have formed in the sample after extrusion, before the size measurements. As the inset of Fig. 1 shows, the number of these large aggregates is negligible.

Due to the small difference between the native liposomes extruded through 50 and 100 nm membranes, we are unable at this stage to comment on the effect of the liposome curvature on the adsorption of SlpA. However, the size distributions of SlpA-containing liposome samples were wider and the average diameter of SlpA-covered liposomes was somewhat larger than that of the respective reference samples for both samples extruded through 50 nm and 100 nm membranes.

The zeta potentials of the SlpA-containing and reference samples differed from each other to some extent (Fig. 2). The zeta potential of reference liposomes was, as expected, positive, although the reference liposome sample extruded through the 50 nm membrane showed a smaller peak at lower potential, indicating an uneven distribution of the positively charged lipids in the liposomes (Fig. 2). The average zeta potential was 34.8 mV for the 100 nm reference sample and 32.6 mV for the 50 nm reference sample.

A shift was observed in the zeta potential of the liposomes by the addition of SlpA (Fig. 2). The maximum of the zeta potential peak shifted to a lower value. The average zeta potential and its standard deviation were 27.1 mV for the liposome sample extruded through the 100 nm membrane and 26.6 mV for the liposome sample extruded through the 50 nm membrane. A shift in the zeta potential indicates a change in the surface charge of the particles in suspension, indicating reassembly of SlpA on the liposomal surface.

For comparison, the zeta potential of SlpA in solution was also measured. Its zeta potential distribution was centered around zero, indicating that the soluble fraction of the protein was prone to rapid aggregation. The comparison of the zeta potentials in Fig. 2 clearly shows that the SlpA-containing liposome sample differed from both the reference liposome samples and SlpA, in terms of measured zeta potential. The data indicate that the SlpA-containing liposome samples are stable and not prone to aggregation at the time of the zeta potential measurements, although some aggregation of proteins may have happened during sample preparation and after the extrusion.

3.2. SAXS results

The SAXS intensities of both SlpA-containing and reference liposome samples shared features related to the liposome structure. Fig. 3 shows the scattering intensities of all samples. The wide maximum at $q = 1\ \mathrm{nm}^{-1}$ is visible in all curves. This maximum corresponds to a Bragg distance of 6 nm and relates to the thickness of the lipid bilayer in the liposomes [26]. A difference between the SlpA-containing and reference samples was evident in the scattering intensity at lower angles, with the scattering intensities starting to diverge at $q < 1\ \mathrm{nm}^{-1}$. This was particularly clearly visible for the sample extruded through the 100 nm membrane.

After subtracting the intensity of the reference sample as background, several peaks were found in the low q-range (Fig. 4). However,

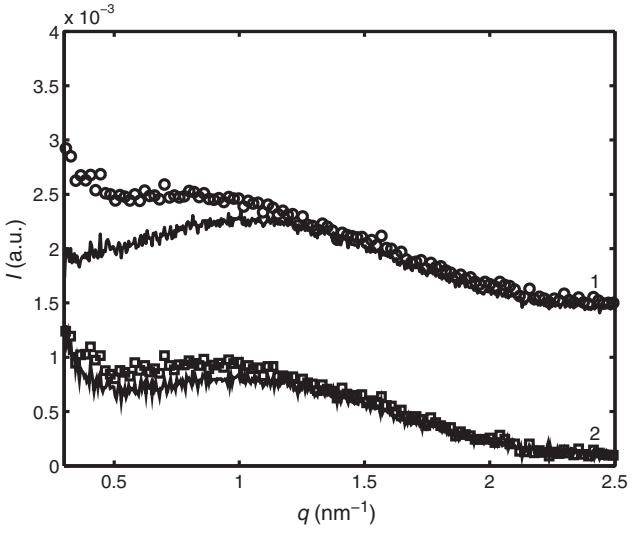

Fig. 3. SAXS intensity as the function of the magnitude of the scattering vector. The scattering intensities of SlpA-containing liposomes extruded through 100 nm (○) or 50 nm membrane (□) are shown together with the intensities of respective reference samples (solid lines). Curves have been vertically shifted for clarity.

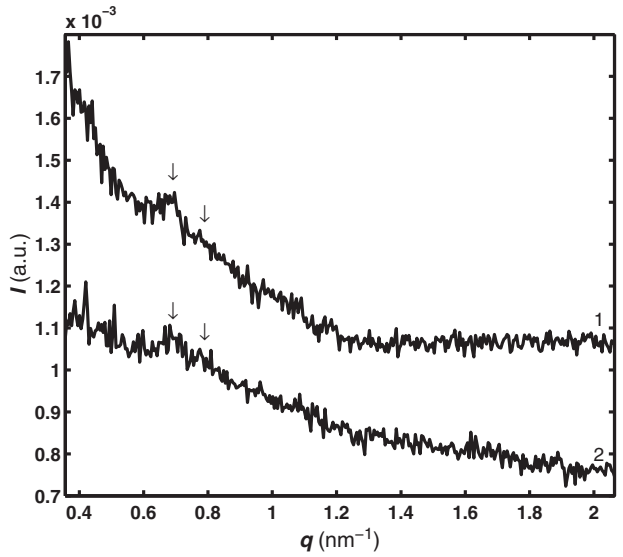

Fig. 4. Scattering intensities of SlpA on liposome samples. Shown are the scattering intensities of SlpA on liposome samples extruded through 100 nm membranes (1) and SlpA on liposome samples extracted through 50 nm membranes (2). Arrows point at diffraction peaks indicating the presence of crystalline structures. Curves have been shifted vertically for clarity.

the concentration of SlpA used was much lower than usually recommended for SAXS — for solution SAXS, concentrations of 1.0–10 mg/ml are typical [27]. Discerning diffraction peaks from the noise peaks with width of one data point is not possible for most peak locations. To obtain better signal-to-noise ratio, samples were centrifuged at 4000 *g* for 10 min, and roughly 80% of the liquid was removed. To subtract the background, the data were normalized in the high *q*-range ($q > 2$ nm^{-1}) and the intensity of the reference sample was subtracted from the intensity of the centrifuged sample, leaving the intensity of SlpA. As seen in Fig. 5, scattering intensities of SlpA from both SlpA-containing samples showed diffraction peaks. The presence of these peaks indicated a good crystalline order in the samples. The diffraction peaks are due to S-layer crystallites on the liposomal surface, as precipitated SlpA does not possess a regular structure (see supporting information). When the diffraction pattern of SlpA-containing liposome samples was compared to the diffraction pattern of SlpA on bacterial cell wall fragments, some diffraction peaks remained in the same position while others had shifted.

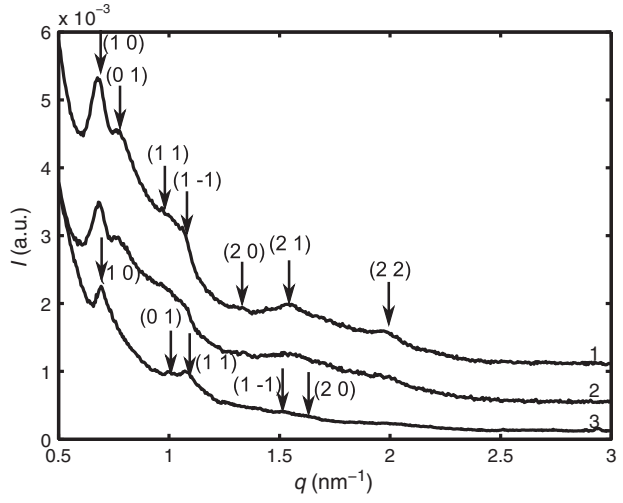

Fig. 5. The scattering intensities of SlpA on SlpA-containing liposomes and native cell wall fragments. Shown are the scattering intensities of SlpA-containing liposomes extruded through 100 nm membranes (1), SlpA-containing liposomes extruded through 50 nm membranes (2), and native cell wall fragments (3). Major reflections are indicated by arrows and corresponding indices. Curves are shifted vertically for clarity.

Both SAXS results and zeta potential measurements indicate that the reassembly was successful. The diffraction pattern indicates that crystallites with regular order in two dimensions were formed. Previously, Hollman et al. have also reported reassemblies of S-layer proteins from *L. kefir* JCM 5818 and *L. brevis* ATCC 14869 on positively charged liposomes [14,28]. The ability of these proteins to reassemble on positively charged surfaces is particularly interesting, as the predicted overall pI values of *Lactobacillus* surface layer proteins are generally high (9.4–10.4) [3]. We also attempted to reassemble SlpA on neutral and negatively charged liposomes (see supporting information) but good crystallites were not formed on these surfaces. Interestingly, the S-layer protein of *L. acidophilus* ATCC 4356 reassembles readily on negatively charged but not on neutral (zwitterionic) lipid monolayers [17]. On the surface of bacteria, the S-layer proteins attach non-covalently to cell wall carbohydrates, which are neutral or negatively charged, and some *Lactobacillus* S-layer proteins bind selectively to e.g. teichoic acids or non-teichoic acid polysaccharides [3]. While the S-layer proteins of *Lactobacilli* share certain common features, such as the high predicted pI and small size, they show a wide variation in their ability to bind to liposomal surfaces of differing surface charge properties.

3.3. The S-layer lattice and crystallite size

The diffraction peaks in the SAXS intensity pattern indicate that the S-layer proteins have formed crystals. For a two-dimensional crystal lattice, a diffraction peak at q_{hk} corresponds to indices h and k and lattice constants a, b, and γ:

$$q_{hk} = \sqrt{\left(\frac{2\pi h}{a\sin\gamma}\right)^2 + \left(\frac{2\pi k}{b\sin\gamma}\right)^2 - 2\left(\frac{2\pi h}{a\sin\gamma}\right)\left(\frac{2\pi k}{b\sin\gamma}\right)\cos(\gamma)}. \quad (1)$$

The lattice constants for the S-layer were calculated from the diffraction pattern by assigning h and k indices to the first diffraction peaks and solving the lattice constants from Eq. (1). The position of the other reflections was monitored and calculations repeated until positions matched observed reflections by fitting diffraction peaks to the scattering intensity. The precision of the positions of the diffraction peaks was determined to be $\Delta q = 0.01$ nm^{-1}. As shown in Fig. 5, the diffraction patterns obtained with SlpA-containing liposomes and native cell walls differed slightly, indicating differences between the SlpA structure on the native cell wall and on the positively charged liposome. For the native S-layer on cell wall fragments, the lattice constants were $a = (9.41 \pm 0.40)$ nm, $b = (6.48 \pm 0.40)$ nm, and $\gamma = (77.0 \pm 2.4)°$. This is in good agreement with the constants previously determined by electron microscopy: $a = 9.39$ nm, $b = 6.10$ nm, and $\gamma = 79.8°$ [22], even though the sample in SAXS measurements consisted of crude cell wall fragments, while the electron microscopy sample was a freeze-etch of a whole bacterial cell. As the accuracy of the EM measurements is ±5% (Dietmar Pum, personal communication), which is very close to the accuracy of the SAXS measurement, we cannot comment on whether the slight difference in lattice constant b results from a real difference in the S-layer on whole bacteria and bacterial cell wall fragments, or whether the lattice constant has changed by 6%. The difference is small and indicates that S-layers are highly stable on the bacterial cell wall.

For the S-layer reassembled on liposomes, the calculation yielded lattice constants of $a = (9.29 \pm 0.33)$ nm, $b = (8.03 \pm 0.33)$ nm, and $\gamma = (84.9 \pm 2.5)°$ for the samples extruded through both 50 nm and 100 nm membranes. The lattice constant a is similar to that obtained with SlpA on cell wall fragments, but the change in lattice constants b and γ are significant. The change in lattice constants is visualized in Fig. 6, with SlpA drawn with p2 symmetry (see supporting information).

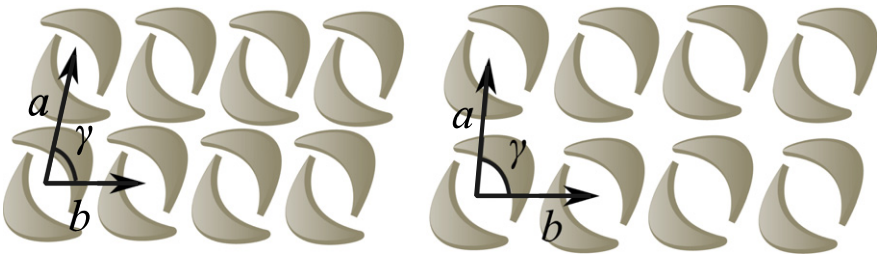

Fig. 6. A schematic representation of the change in the lattice constants of arrays of SlpA. Shown are native SlpA on cell wall fragments (left) and SlpA reassembled on liposomes (right).

The crystal size s of the S-layer was determined using Scherrer's formula:

$$s = \frac{0.9\lambda}{\sqrt{(\Delta 2\theta)^2 - (\Delta 2\theta_{inst})^2}\cos\theta}, \quad (2)$$

where λ is the wavelength of the radiation, $\Delta 2\theta$ the full width at half maximum (FWHM) of the reflection and θ half of the scattering angle 2θ. As the instrumental broadening $\Delta 2\theta_{inst}$ for the linewidth was unknown, the crystallite size was calculated twice to get an upper and lower limit for crystallite size. The lower limit of crystallite size was calculated by setting the instrumental broadening as zero, and the upper limit by using the FWHM of the (001) reflection of the silver behenate (0.036 nm^{-1}) as the instrumental broadening.

Determined from the FWHM of the (10) reflection (0.065 nm^{-1}), the crystallite size for the 100 nm POPC/DOTAP sample was 92 nm < s < 114 nm. This corresponds approximately to the length of ten unit cells in the corresponding direction. This peak is clearly the best defined of the diffraction peaks, and the size of the crystal in other directions could not be reliably determined.

The liposome dimensions are significantly smaller than those of a bacterium. When using SAXS to study the S-layer of whole bacteria, Sekot et al. [9] found crystallite sizes corresponding to twenty unit lengths, or 300 nm, for the S-layer of *Aquaspirillum serpens* MW5, indicating that even on the native surface, the S-layer does not form a continuous crystal. In this study, the crystallite size is significant when compared to the liposome size, but does not indicate that a single crystal would cover the circumference of the liposome even at its longest dimension, as the DLS measurements indicate that the average diameter of SlpA covered liposomes is 113–148 nm depending on the pore size of the membrane. This corresponds to a circumference of 360–460 nm.

At 100 nm, the crystallite size corresponds to approximately ten unit cell lengths in the direction of lattice constant a. As this corresponds to the direction where lattice constants remained unchanged, it indicates that the S-layer is most stable in this direction. The other direction, b, has fewer units aligned, and also changed significantly in the reassembly. These changes may be related: the protein molecule, while interacting with the liposome surface, adopts a slightly different conformation, leading to an increase in b and a reduced tendency for symmetry in this direction. Whether this is due to the curvature of the liposome surface or its surface charge properties could not be determined.

4. Conclusions

The S-layer protein SlpA of *L. brevis* ATCC 8287 was found to reassemble on positively charged liposomes. Both SAXS measurements and zeta potential measurements supported this conclusion. The self-assembly could be seen from the SAXS intensity as a difference in the intensity in the low q-range, with clear diffraction peaks indicating that the reassembly is crystalline.

We showed that SAXS is a useful technique in characterizing the properties of crystalline structure formed by S-layer proteins, and with a synchrotron source, even dilute samples (SlpA concentration < 0.2 mg/ml) could be measured. The lattice constants determined from the SAXS intensity of bacterial cell wall fragments, $a = 9.41$ nm, $b = 6.48$ nm, and $\gamma = 77.0°$, corresponded very well to the lattice constants previously determined by electron microscopy. The agreement of the average structure determined by SAXS and the local structure determined by electron microscopy supports the use of SAXS to study S-layers, and shows that on the bacterial cell surface, the S-layer is very stable as differences in sample preparation did not seem to influence the structure.

While the S-layer is very stable on the cell surface, it does not reassemble to exactly the same structure on all surfaces. SAXS has a resolution that allows for monitoring changes in lattice constants, and different sample types can easily be compared. We discovered that one of the lattice constants determined for SlpA reassembled on positively charged liposomes had changed compared to the native state: the shorter lattice constant b had increased by 24% (1.6 nm) while the change in the longer lattice constant a was negligible. From the diffraction pattern, the size of the crystallite was calculated to be around 100 nm in [10] direction, but as the other diffraction peaks were wider and less well defined, the corresponding crystallite size could not be calculated. As the lattice constant a remained unchanged, both the crystallite size and the lattice constants indicated better stability of the reassembly in this direction.

Acknowledgments

The authors thank Erno Karjalainen for help with the DLS and zeta potential measurements, Dr. Mika Torkkeli and Pentti Jääskeläinen for SAXS measurements of native cell wall fragments and Dr. Tomas Plivelic and Dr. Ana Labrador for help with experiments at I911-SAXS.

The research leading to these results has received funding from the European Community's Seventh Framework Programme (FP7/2007–2013) CALIPSO under grant agreement no. 312284. Support from the Vilho, Yrjö and Kalle Väisälä's fund (IK), the Academy of Finland (133186) (IK) and the Magnus Ehrnrooth Foundation (SKW) is gratefully acknowledged.

Appendix A. Supplementary data

Supplementary data to this article can be found online at http://dx.doi.org/10.1016/j.bbamem.2014.04.022.

References

[1] M. Sára, U.B. Sleytr, S-layer proteins, J. Bacteriol. 182 (2000) 859–868, http://dx.doi.org/10.1128/JB.182.4.859-868.2000.
[2] U.B. Sleytr, T.J. Beveridge, Bacterial S-layers, Trends Microbiol. 7 (1999) 253–260, http://dx.doi.org/10.1016/S0966-842X(99)01513-9.
[3] U. Hynönen, A. Palva, *Lactobacillus* surface layer proteins: structure, function and applications, Appl. Microbiol. Biotechnol. 97 (2013) 5225–5243, http://dx.doi.org/10.1007/s00253-013-4962-2.
[4] E.S. Györvary, O. Stein, D. Pum, U.B. Sleytr, Self-assembly and recrystallization of bacterial S-layer proteins at silicon supports imaged in real time by atomic force microscopy, J. Microsc. 212 (2003) 300–306, http://dx.doi.org/10.1111/j.1365-2818.2003.01270.x.
[5] S.-H. Shin, S. Chung, B. Sanii, L.R. Comolli, C.R. Bertozzi, J.J.D. Yoreo, Direct observation of kinetic traps associated with structural transformations leading to multiple

pathways of S-layer assembly, Proc. Natl. Acad. Sci. 109 (2012) 12968–12973, http://dx.doi.org/10.1073/pnas.1201504109.
[6] J.L. Toca-Herrera, S. Moreno-Flores, J. Friedmann, D. Pum, U.B. Sleytr, Chemical and thermal denaturation of crystalline bacterial S-layer proteins: an atomic force microscopy study, Microsc. Res. Tech. 65 (2004) 226–234, http://dx.doi.org/10.1002/jemt.20127.
[7] H. Vilen, U. Hynönen, H. Badelt-Lichtblau, N. Ilk, P. Jääskeläinen, M. Torkkeli, et al., Surface location of individual residues of SlpA provides insight into the *Lactobacillus brevis* S-layer, J. Bacteriol. 191 (2009) 3339–3349, http://dx.doi.org/10.1128/JB.01782-08.
[8] C. Horejs, D. Pum, U.B. Sleytr, H. Peterlik, A. Jungbauer, R. Tscheliessnig, Surface layer protein characterization by small angle X-ray scattering and a fractal mean force concept: from protein structure to nanodisk assemblies, J. Chem. Phys. 133 (2010), http://dx.doi.org/10.1063/1.3489682 (175102/1–8).
[9] G. Sekot, D. Schuster, P. Messner, D. Pum, H. Peterlik, C. Schäffer, SAXS for imaging of S-layers on intact bacteria in native environment, J. Bacteriol. (2013) 2408–2414, http://dx.doi.org/10.1128/JB.02164-12.
[10] V.P. Torchilin, Recent advances with liposomes as pharmaceutical carriers, Nat. Rev. Drug Discov. 4 (2005) 145–160, http://dx.doi.org/10.1038/nrd1632.
[11] D. Felnerova, J.-F. Viret, R. Glück, C. Moser, Liposomes and virosomes as delivery systems for antigens, nucleic acids and drugs, Curr. Opin. Biotechnol. 15 (2004) 518–529, http://dx.doi.org/10.1016/j.copbio.2004.10.005.
[12] B. Schuster, U.B. Sleytr, S-layer-supported lipid membranes, Rev. Mol. Biotechnol. 74 (2000) 233–254, http://dx.doi.org/10.1016/S1389-0352(00)00014-3.
[13] C. Mader, S. Küpcü, M. Sára, U. Sleytr, Stabilizing effect of an S-layer on liposomes towards thermal or mechanical stress, Biochim. Biophys. Acta Biomembr. 1418 (1999) 106–116, http://dx.doi.org/10.1016/S0005-2736(99)00030-9.
[14] A. Hollmann, L. Delfederico, G. Glikmann, G. De Antoni, L. Semorile, E.A. Disalvo, Characterization of liposomes coated with S-layer proteins from lactobacilli, Biochim. Biophys. Acta Biomembr. 1768 (2007) 393–400, http://dx.doi.org/10.1016/j.bbamem.2006.09.009.
[15] C. Mader, S. Küpcü, U.B. Sleytr, M. Sára, S-layer-coated liposomes as a versatile system for entrapping and binding target molecules, Biochim. Biophys. Acta Biomembr. 1463 (2000) 142–150, http://dx.doi.org/10.1016/S0005-2736(99)00190-X.
[16] D. Schuster, S. Küpcü, D.J. Belton, C.C. Perry, M. Stöger-Pollach, U.B. Sleytr, et al., Construction of silica-enhanced S-layer protein cages, Acta Biomater. 9 (2013) 5689–5697, http://dx.doi.org/10.1016/j.actbio.2012.11.015.
[17] E. Smit, F. Oling, R. Demel, B. Martinez, P.H. Pouwels, The S-layer protein of *Lactobacillus acidophilus* ATCC 4356: identification and characterisation of domains responsible for S-protein assembly and cell wall binding, J. Mol. Biol. 305 (2001) 245–257, http://dx.doi.org/10.1006/jmbi.2000.4258.
[18] E. Rönkä, E. Malinen, M. Saarela, M. Rinta-Koski, J. Aarnikunnas, A. Palva, Probiotic and milk technological properties of *Lactobacillus brevis*, Int. J. Food Microbiol. 83 (2003) 63–74, http://dx.doi.org/10.1016/S0168-1605(02)00315-X.
[19] S. Åvall-Jääskeläinen, K. Kylä-Nikkilä, M. Kahala, T. Miikkulainen-Lahti, A. Palva, Surface display of foreign epitopes on the *Lactobacillus brevis* S-Layer, Appl. Environ. Microbiol. 68 (2002) 5943–5951, http://dx.doi.org/10.1128/AEM.68.12.5943-5951.2002.
[20] U. Hynönen, B. Westerlund-Wikström, A. Palva, T.K. Korhonen, Identification by flagellum display of an epithelial cell- and fibronectin-binding function in the SlpA surface protein of *Lactobacillus brevis*, J. Bacteriol. 184 (2002) 3360–3367, http://dx.doi.org/10.1128/JB.184.12.3360-3367.2002.
[21] P. Mobili, A. Londero, T.M.R. Maria, M.E.S. Eusébio, G.L. De Antoni, R. Fausto, et al., Characterization of S-layer proteins of *Lactobacillus* by FTIR spectroscopy and differential scanning calorimetry, Vib. Spectrosc. 50 (2009) 68–77, http://dx.doi.org/10.1016/j.vibspec.2008.07.016.
[22] S. Åvall-Jääskeläinen, U. Hynönen, N. Ilk, D. Pum, U. Sleytr, A. Palva, Identification and characterization of domains responsible for self-assembly and cell wall binding of the surface layer protein of *Lactobacillus brevis* ATCC 8287, BMC Microbiol. 8 (2008) 165, http://dx.doi.org/10.1186/1471-2180-8-165.
[23] Avanti Polar Lipids, http://avantilipids.com/ Jan. 21, 2014.
[24] F. Bordi, C. Cametti, C. Di Venanzio, S. Sennato, S. Zuzzi, Influence of temperature on microdomain organization of mixed cationic–zwitterionic lipidic monolayers at the air–water interface, Colloids Surf. B: Biointerfaces 61 (2008) 304–310, http://dx.doi.org/10.1016/j.colsurfb.2007.09.010.
[25] A. Labrador, Y. Cerenius, C. Svensson, K. Theodor, T. Plivelic, The yellow mini-hutch for SAXS experiments at MAX IV Laboratory, J. Phys. Conf. Ser. 425 (2013) 072019, http://dx.doi.org/10.1088/1742-6596/425/7/072019.
[26] T. Viitala, J.T. Hautala, J. Vuorinen, S.K. Wiedmer, Structure of anionic phospholipid coatings on silica by dissipative quartz crystal microbalance, Langmuir 23 (2007) 609–618, http://dx.doi.org/10.1021/la060923t.
[27] EMBL Hamburg, biological small angle scattering, http://www.embl-hamburg.de/biosaxs/ Jan. 21, 2014.
[28] A. Hollmann, L. Delfederico, G. De Antoni, L. Semorile, E.A. Disalvo, Interaction of bacterial surface layer proteins with lipid membranes: synergysm between surface charge density and chain packing, Colloids Surf. B: Biointerfaces 79 (2010) 191–197, http://dx.doi.org/10.1016/j.colsurfb.2010.03.046